

1 **Whistling shares a common tongue with speech: Bioacoustics from**
2 **real-time MRI of the human vocal tract**

3 Michel Belyk^{1,2,3}, Benjamin G. Schultz^{3,4}, Joao Correia^{3,5}, Deryk S. Beal^{2,6},
4 Sonja A. Kotz^{3,7}

5 ¹Department of Speech, Hearing and Phonetics, University College London,
6 UK.

7
8 ²Bloorview Research Institute, Holland Bloorview Kids Rehabilitation Hospital,
9 Toronto, Canada

10
11 ³Faculty of Psychology and Neuroscience, University of Maastricht,
12 Maastricht, The Netherlands

13
14 ⁴Institute of Logic, Language, & Computation, University of Amsterdam,
15 Amsterdam, The Netherlands

16
17 ⁵Basque Center on Cognition, Brain and Language, Donostia-San Sebastian,
18 Spain.

19
20 ⁶Department of Speech-Language Pathology, University of Toronto, Toronto,
21 Canada

22
23 ⁷Department of Neuropsychology, Max Planck Institute for Human and
24 Cognitive Sciences, Leipzig, Germany

25 **RUNNING TITLE: Bioacoustics of whistling**

26 **Keywords: whistle, speech, communication, tongue, magnetic resonance**
27 **imaging, evolution**

28

29 *Correspondence to:*

30 Michel Belyk, Ph.D.

31 University College London

32 Speech, Hearing and Phonetic Sciences

33 London, United Kingdom

34 e-mail: belykm@gmail.com

35
36

Abstract

37 Most human communication is carried by modulations of the voice. However,
38 a wide range of cultures has developed alternate forms of communication that
39 make use of a whistled sound source. For example, whistling is used as a
40 highly salient signal for capturing attention, can have iconic cultural meanings
41 such as the cat-call, enact a formal code as in boatswain's calls, or stand as a
42 proxy for speech in whistled languages. We used real-time magnetic
43 resonance imaging to examine the muscular control of whistling to describe a
44 strong association between the shape of the tongue and the whistled
45 frequency. This bioacoustic profile parallels the use of the tongue in vowel
46 production. This is consistent with the role of whistled languages as proxies
47 for spoken languages, in which one of the acoustical features of speech
48 sounds are substituted with a frequency modulated whistle. Furthermore,
49 previous evidence that non-human apes may be capable of learning to whistle
50 from humans suggests that these animals may have similar sensorimotor
51 abilities to those that are used to support speech in humans.

52

Introduction

53 Whistling produces a loud and pitched sound that approximates a sine-wave.
54 These sounds travel well over large distances [1] and are easy to discern from
55 other biological sounds by the rare occurrence of pure tone sine waves in
56 nature. These features have made whistling a viable alternative sound source
57 for human communication when signal fidelity may be more important than
58 signal complexity [2,3].

59 Whistling may be a more robust channel in contexts where the voice is
60 unreliable, such as communication over long distances or in poor weather.
61 For example, naval vessels maintain a traditional code of boatswain's calls, in
62 which arbitrary combinations of whistles correspond to simple commands
63 [4,5]. Furthermore, a number of cultures have developed whistled proxies of
64 spoken language [6]. In these languages, the whistled frequency stands in for
65 one of the acoustical features that would normally be carried by the voice [6–
66 8]. Whistled languages encode less information from which to identify the
67 intended speech sounds than voiced speech, but are more robust to long
68 distance communication. The narrow frequency band of the whistle gives it
69 more power per unit of spectral bandwidth, increasing its signal-to-noise ratio
70 and the effective range of communication [1–3].

71 Whistles are physical phenomena that occur when airflow interacts with
72 objects to produce a positive feedback loop. For example, the hole-tone
73 whistle is produced when a jet of air passes through two constrictions [9,10].
74 The space between the constrictions forms a resonator that selectively
75 amplifies particular frequencies. Pressure fluctuations at the surface of the jet

76 propagate backwards and are amplified according to the characteristics of the
77 resonator. 11,12]. Ring-shaped vortexes are formed in the downstream jet at
78 the frequency of the resonant cavity. The perceptual property of this periodic
79 waveform is the pitch of the whistle.

80 Many whistled codes used by humans are produced with the aid of the hands
81 or an instrument, but the most basic form of whistling is the bilabial whistle.
82 Though common knowledge suggests that whistling is primarily determined by
83 the action of the lips, the tongue has an active role. Shadle [11] hypothesised
84 that the lips form a constriction through which a jet of air is forced and that a
85 resonant cavity behind the lips and bounded by the tongue determines the
86 frequency that is whistled.

87 The tongue is a muscular organ that is divided into extrinsic and intrinsic
88 muscle groups [13,14]. The extrinsic lingual muscles originate in osseous
89 structures, such as the mandible and hyoid bone, and insert in the body of the
90 tongue with the primary function of changing the tongue's position. The
91 intrinsic lingual muscles make up the body of the tongue itself and serve to
92 reconfigure the shape of the tongue to produce the dexterous movements
93 required by both swallowing and speech. The human tongue in particular
94 receives dense and complex innervation, which may support fine motor-
95 control [15–17]. The changing shape of the tongue is used during speech to
96 create narrow constrictions in the oral cavity that divide the vocal tract into a
97 series of resonant cavities [18–20]. Together these cavities selectively amplify
98 a combination of frequency bands that encode vowel sounds of speech [20–
99 22].

100 Two previous studies provide support for the role of the tongue in whistling.
101 Kaburagi et al. [23] used magnetic resonance imaging to gather still images of
102 one individual. Qualitatively, it appeared from these images that the
103 configuration of the tongue varied by the frequency being whistled with gross
104 similarity to vowel production. Azola et al. [24] gathered x-ray cineradiographic
105 images from two individuals providing evidence that the space between the tip
106 of the tongue to the incisors forms a resonant cavity as with speech.

107 We used real-time anatomical MRI to collect videographic data with high
108 contrast between the tongue and the surrounding vocal tract. We modeled the
109 cross-sectional shape of the tongue to quantify tongue movements in their
110 entirety and applied functional principle components analysis to explore
111 variation in the tongue shapes that whistlers employed. This approach
112 provided a quantitative, generalizable, and holistic description of the tongue's
113 role in whistling.

114 **Methods**

115 *Participants*

116 Six participants (three male, including authors MB and BS) with no speech-
117 motor or auditory deficits were recruited from Maastricht University.
118 Participants had varied cultural backgrounds including German, Dutch,
119 Canadian, Australian, and American and ages ranging from 20 to 33.

120 *Procedure*

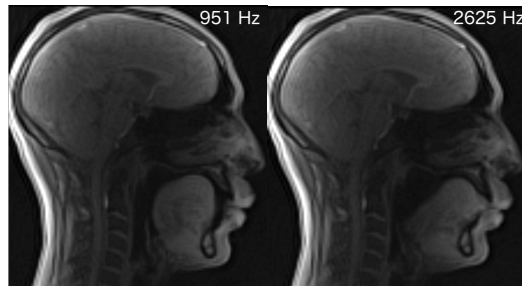
121 Each participant performed three sound production tasks while undergoing
122 real-time magnetic resonance imaging (rtMRI). In separate runs, each
123 participant was instructed to 1) whistle a continuous siren spanning the range

124 of frequencies that they could reliably produce, 2) whistle a chromatic scale of
125 discrete notes over the same range, and 3) produce a whistle with
126 conventionalized meaning (a “cat call” was familiar to all participants despite
127 diverse cultural backgrounds). Participants were instructed to produce sound
128 as part of a breath phrase of approximately eight seconds and to breathe
129 normally. Participant’s heads were constrained by foam pillows in the MRI.

130 *Real-time magnetic resonance imaging*

131 Real-time MRI collects a series of anatomical images from a mid-sagittal slice
132 of the head and neck (Figure 1). Images were collected on a Siemens 3T
133 MAGNETOM Prisma Fit at the Maastricht Brain Imaging Centre with the
134 LiveView pulse sequence [25]. T1-weighted images were collected with an
135 acquisition time of 60ms (sampling rate 16.67 Hz) over a single mid-sagittal
136 slice with thickness = 8 mm, in-plane resolution = 2 mm by 2 mm, field-of-view
137 = 256 by 256 mm, repetition time = 2.58 ms, echo time = 1.64 ms, and flip
138 angle = 8°. K-space was sampled over 125 radial spokes. Scan durations
139 were controlled manually and ranged from 88 to 98 seconds per run. Two
140 runs (call, discrete scale) from one participant were discarded due to scanner
141 malfunction or poor signal-to-noise ratio in imaging data. A third run (discrete
142 scale) from a separate participant was discarded due to poor audio recording
143 quality.

144



145

146 Figure 1: Still images of the highest and lowest frequency whistled by one
147 participant whistling a continuous siren.

148

149 *Acoustical measurement*

150 Audio recordings were collected continuously throughout the scanning
151 session using an MRI compatible microphone attached to the side of the head
152 coil (sampling frequency 44100 Hz, quantization 32-bit). Recordings were
153 anti-alias filtered by applying a low-pass filter at the sampling frequency prior
154 to digitization. Audio and rtMRI data were synchronised by aligning the onset
155 of acoustical artefacts associated with MRI acquisition with the first image
156 volume.

157 Acoustical MRI artefacts were then removed using the noise reduction
158 algorithm in Audacity [26]. The spectral profile of the MRI acoustical artefact
159 was estimated from a period after the onset of the MRI related noise in each
160 scanning run and before the onset of whistling and this noise component was
161 down-weighted across the recording (noise reduction = 48 dB, sensitivity =
162 1.5, frequency smoothing = 3 bands). Two iterations of this procedure
163 sufficiently filtered the acoustical waveform. Recorded waveforms were
164 visually inspected in Praat (v6.0.36) [27] by an experienced acoustical analyst
165 (MB) to identify remaining artefacts and omit corresponding time points from
166 further analysis.

167 Whistling frequency measurements were extracted semi-automatically with an
168 in-house Praat script. The script extracted the fundamental frequency by
169 autocorrelation and calculated the mean frequency within a window equal to
170 half the rtMRI sampling rate centered at each image acquisition.

171 *Tongue shape measurement*

172 The edge of the tongue was detected in each frame automatically using a
173 custom MATLAB script [28,29]. A trace was then computed from tongue-edge
174 maps using the tongue root as a reliably identifiable point of origin. This
175 produced a continuous function of Y (anterior-posterior) and Z (ventral-dorsal)
176 coordinates that capture the shape of the tongue. The coordinate values were
177 centered to create an image space with the origin at the center of mass of the
178 tongue in each frame for analytical purposes. Figures are plotted with origins
179 at the tongue root to facilitate visualization.

180 *Functional data analysis*

181 Spatially smooth representations of the tongue contour were created by
182 modeling each tongue trace with a B-spline with a basis set of cubic
183 polynomials placed at every second sample along the trace using the *fda*
184 package implemented in R [30,31]. Smoothing parameters were chosen by
185 generalised cross validation. The length of each trace was normalised to the
186 mean to remove the confounding influence of the cross-sectional size of the
187 tongue and to ensure that tongue splines were modeled with a consistent
188 number of knots.

189 Variation in tongue shape was explored using functional principal components
190 analysis (fPCA) [32]. Functional PCA explores patterns of variation in the
191 shapes of functions around a mean shape [33]. Much like discrete PCA, fPCA
192 seeks principal components that maximize variation between observations
193 [34–36]. The principal components of discrete PCA are eigenvectors that map
194 each component back onto a set of discrete variables. The principal
195 components of functional PCA are eigenfunctions that map each component
196 back onto variations in shape (Supplementary file 1). FPCA was conducted
197 simultaneously on functions of Y and Z coordinates to produce a two-
198 dimensional description of tongue shape variation. This approach has the
199 benefit of partitioning anterior-posterior (Y) and dorsal-ventral (Z) functions
200 and yields separate Y and Z principal component subscores. These
201 subscores can be interpreted as the degree to which the shape of tongue is
202 deformed along the Y or Z plane in each MRI frame.

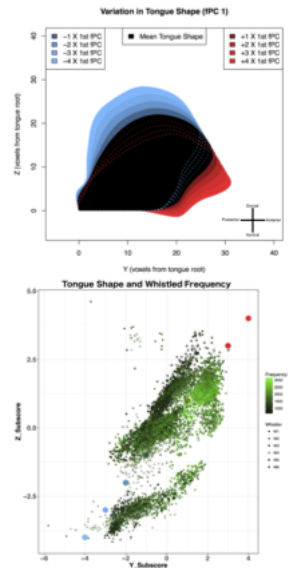
203 A separate examination of the functional principal components for each
204 participant and each whistling task confirmed that the components were highly
205 consistent across participants and tasks. The data were therefore combined
206 and fitted to a linear mixed-effects model with the dependent variable of
207 whistled frequency, with Y and Z subscores as regressors. The model
208 accounted for random factors of Participant and Condition with random slopes
209 for the effects Y and Z subscores at each level of the random factors [37].
210 This approaches the maximal random effects structure [38], though random
211 effects of Condition were not nested within Participant due to a failure of more
212 complex models to converge [$\text{Hz} \sim 1 + Y * Z + (1 + Y * Z \mid \text{Whistler}) + (1 + Y * Z \mid$
213 $\text{Condition})$]. Significance was assessed by *F*-tests with degrees of freedom

214 determined by Satterthwaite's approximation for degrees of freedom, at an
215 alpha level of 0.05.

216 **Results**

217 The first two functional principal components (fPC) accounted for 62% and
218 17% of the total variance in tongue contour. These functional components
219 describe a dimension from 1) low-forward to high-back tongue position and 2)
220 high-forward to low-back tongue position (Figures 2 and 3). As each fPC
221 describes a distinct dimension of tongue shapes, we report separate models
222 for each principal component. Across both fPCs Y subscores were clearly
223 associated with whistled frequency. Supplementary materials 2-4 contain
224 representative MR videography clips synced with audio. This relationship is
225 summarised by the β parameters reported below. These indicate the increase
226 in whistled frequency per increase of 1 unit of fPC score (equivalent to
227 adjacent tongue shapes in Figures 2 and 3).

228 Y subscores on the first functional principal component predicted the
229 frequency that was being whistled ($F(1, 8.5) = 6.5, p = 0.03, \beta = 399.1, CI =$
230 $[92.9, 705.3]$). Z subscores were poor predictors of whistled frequency ($F(1,$
231 $5.5) = 2.1, p = 0.21, \beta = -200.1, CI = [-473.5, 75.3]$), and no interaction was
232 apparent between subscores ($F(1, 8.4) = 0.01, p = 0.94, \beta = 4.5, CI = [-112.1,$
233 $121.0]$). An anterior-ventral tongue position was associated with high
234 frequency whistling ($R^2 = 0.61$; Figure 2).

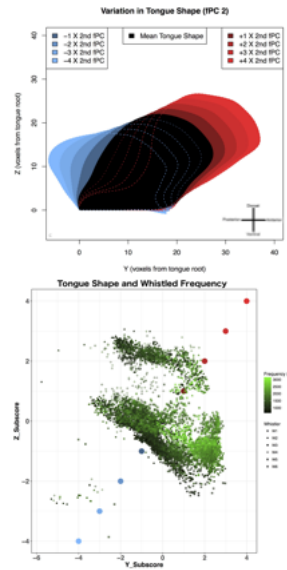


235

236 Figure 2: Top) Mean shape of the tongue (black) framed by shapes marking
 237 the first functional principle component (red to blue). Successive shades of
 238 red mark tongue shapes with fPC1 scores of +1 to + 4. Successive shades of
 239 blue mark tongue shapes with fPC1 scores of -1 to -4. Dashed lines continue
 240 each shaded area where they would otherwise be obscured. Bottom)
 241 Scatterplot showing Y and Z subcomponent scores of fPC1 for each frame.
 242 Colour hue indicates the frequency being whistled at each frame. Symbols
 243 indicate the whistler that contributed each point. Large background circles are
 244 fictive data points plotted for the purpose of facilitating the interpretation of
 245 fPC scores only. Each fictive point indicates the fPC1 score associated with
 246 the tongue shape of the same colour in the top panel. The origin corresponds
 247 to the mean tongue shape.

248

249 Y subscores on the second functional principal component also predicted the
 250 frequency that was being whistled ($F(1, 8.8) = 5.8, p = 0.04, \beta = 297.0, CI =$
 251 $[56.2, 537.8]$). Z subscores were poor predictors of whistled frequency ($F(1,$
 252 $5.6) = 1.9, p = 0.22, \beta = 222.7, CI = [-96.5, 541.8]$) and no interaction was
 253 apparent between subscores ($F(1, 8.6) = 0.04, p = 0.84, \beta = 13.8, CI = [-$
 254 $115.2, 142.8]$). An anterior-dorsal tongue position was associated with high
 255 frequency whistling ($R^2 = 0.60$; Figure 3).



256

257 Figure 3: Top) Mean shape of the tongue framed by shapes describing the
 258 second functional principle component. Bottom) Scatterplot showing Y and Z
 259 subcomponent scores of fPC2 for each frame.

260

Discussion

261 We used rtMRI to demonstrate that the shape of the tongue is strongly
 262 associated with the frequency of bilabial whistling in humans, such that
 263 forward configuration of the tongue produced the highest frequencies
 264 regardless of tongue height. This mechanism was consistent across contexts,
 265 including simple but highly artificial siren sounds, music-like discrete
 266 chromatic scales, and complex calls with culturally imposed meaning. This is
 267 consistent with Shadle's hypothesis that the tongue shapes a resonant cavity
 268 behind the lips to determine the whistled frequency [11]. Tongue
 269 configurations that reduce the size of the resonant cavity between the incisors
 270 and the tongue amplify pressure fluctuations with shorter wavelengths (i.e.,
 271 higher frequencies). Our approach modeled the entire cross sectional surface
 272 of the tongue. Though the posterior tongue may be ancillary to whistled sound
 273 production, its movement is none the less a part of whistled sound production.

274

275 *A shared bioacoustical mechanism with speech*

276 The same mechanism determines the frequency of whistling and the identities
277 of spoken vowels. Vowel sounds are produced by shaping resonant cavities
278 within the vocal tract [19,20,32]. These resonant cavities selectively amplify
279 certain frequency bands of the voice, called formants, which together encode
280 the identity of spoken vowels [18,39]. For, example a low-back tongue
281 position produces a high first formant (F1) and low second formant (F2), as in
282 the sound /ɑ/ (odd). A high-forward tongue position produces a low F1 and
283 high F2, as in the sound /i/ (even). The most anterior of these resonant
284 cavities, which determines the second formant in the context of speech, is a
285 strong driver of whistled frequency. We observed whistled frequencies
286 ranging from 600 Hz to 3100 Hz, which spans the values of the second
287 formant that encode vowel sounds [40–42].

288 We observed two functional principal components of tongue shape: One
289 capturing variation from low-back to high-forward tongue configurations and a
290 second capturing variation from high-back to low-forward tongue
291 configurations. Forward configurations of the tongue were associated with
292 high frequencies across components, suggesting that multiple tongue
293 configurations may produce similar bioacoustical effects. These alternative
294 modes of production may provide an avenue to study motoric degrees of
295 freedom in this muscular system [43].

296 The shared bioacoustics of whistling and vowel production may inform the
297 study of whistled languages. Twelve whistled languages have been
298 documented, though anecdotal reports suggest that they may be more
299 abundant [2,6]. The most well studied of these is Silbo Gomero of the Canary

300 Islands, in which whistling is used as a sound source in place of the voice
301 [44]. Silbadors produce loud hand-assisted whistles to communicate over long
302 distances over mountainous terrain. They describe producing Silbao as
303 whistling while moving ones tongue as though to pronounce words in spoken
304 Spanish [44]. The effect is to approximate spoken Spanish with the whistled
305 frequency standing in for the second formant (F2) of Spanish vowels [6,7].
306 Similar whistled-proxies have been described of French [45], Turkish [46], and
307 Greek [47], among other languages [2,6]. Though the simpler acoustical
308 structure of whistling encodes less information than the voice, even amateur
309 whistlers are highly precise [48]. The common bioacoustical mechanisms of
310 speaking and whistling may explain the emergence of whistled proxies across
311 diverse languages and cultural groups.

312 *A bioacoustical clue to the evolution of speech*

313 Whistling may provide a novel avenue to understand the evolution of speech
314 motor abilities through the comparative study of human and non-human apes.
315 Though whistling has not been observed in non-human apes in the wild, at
316 least one species (*Pongo* spp.) can learn to whistle in captivity [49,50]. In
317 most instances it has not been possible to determine whether these animals
318 spontaneously imitated their caretakers or were explicitly trained. In one case,
319 this behaviour was observed to transfer between cohabitating animals,
320 demonstrating the potential for cultural transmission [49]. This behaviour has
321 provided evidence that orangutans have voluntary control over the upper lip,
322 lower-lip, and respiratory muscles, which are readily accessible to external
323 observation. Our study, along with that of Azola et al. [24], demonstrates the
324 strong involvement of the tongue in human bilabial whistling. Whistling in non-

325 human apes may provide a useful animal model for the study of sensorimotor
326 capacities that support speech. Dynamic imaging in non-human apes is
327 needed to confirm that the tongue is similarly involved when these species
328 whistle, in line with broad similarities in vocal tract anatomy [51].

329

Conclusions

330 The tongue is a strong determinant of the frequency of oral whistling, with
331 forward tongue configurations associated with higher frequencies. This lingual
332 component of whistling corresponds with the bioacoustical mechanism that
333 produces the second formant in vowel production. This finding is consistent
334 with the link between whistled languages and the spoken languages for which
335 they act as proxy. Comparative research with non-human apes that have
336 learned to whistle may provide further insights into the evolution of the lingual-
337 motor skills that support speech.

338 **Ethics**

339 This study was approved by the Ethical Review Committee for Psychology and Neuroscience
340 at Maastricht University.

341

342 **Data Accessibility**

343 Data and code are available from the Dryad repository (doi.org/10.5061/dryad.kb56cd1).

344

345 **Author Contributions**

346 M.B. conceived of the study, designed the study, analysed the data, and drafted the
347 manuscript; B.G.S and J.C. helped design the study and provided analytical support, D.B.
348 contributed to drafting the manuscript. S.A.K. contributed to the design of the study. All
349 authors contributed comments and critical revisions.

350 **Competing Interests**

351 The authors report no competing interests.

352

353 **Funding**

354 This work was funded by grants from the Natural Sciences Research Council of Canada
355 [PDF502954-2017] and the Kimmel Family Opportunity Fund, and the Biotechnical and
356 Biological Sciences Research Council of the UK [BB/M009742/1].

357

358 **Acknowledgements**

359 We thank Nicolas Iuorio for engineering support.

360 **Figure Legends**

361

362

363

References

- 364 1. Wiley RH, Richards DG. 1978 Physical constraints on acoustic
365 communication in the atmosphere: Implications for the evolution of
366 animal vocalizations. *Behav. Ecol. Sociobiol.* **3**, 69–94.
367 (doi:10.1007/BF00300047)
- 368 2. Meyer J. 2004 Bioacoustics of human whistled languages: An
369 alternative approach to the cognitive processes of language. *An. Acad.*
370 *Bras. Cienc.* **76**, 405–412. (doi:/S0001-37652004000200033)
- 371 3. Meyer J. 2005 Whistled speech: A natural phonetic description of
372 languages adapted to human perception and to the acoustical
373 environment. In *9th European Conference on Speech Communication*
374 *and Technology*, pp. 49–52.
- 375 4. Manwaring GE. 1922 The boatswains whistle. *Mar. Mirror* **8**, 98–101.
376 (doi:10.1080/00253359.1922.10655133)
- 377 5. Lieutenant A. 1911 The boatswain's call. *Mar. Mirror* **1**, 9–15.
378 (doi:10.1080/00253359.1911.10654462)
- 379 6. Rialland A. 2005 Phonological and phonetic aspects of whistled
380 languages. *Phonology* **22**, 237–271.
381 (doi:10.1017/S0952675705000552)
- 382 7. Meyer J. 2008 Typology and acoustic strategies of whistled languages:
383 Phonetic comparison and perceptual cues of whistled vowels. *J. Int.*
384 *Phon. Assoc.* **38**, 69–94. (doi:10.1017/S0025100308003277)
- 385 8. Shadle CH. 1981 The acoustics of whistling. *J. Acoust. Soc. Am.* **70**,
386 S12. (doi:10.1119/1.2341241)
- 387 9. Chanaud RC. 1970 Aerodynamic whistles. *Sci. Am.* **222**, 40–47.
- 388 10. Wilson TA, Beavers GS, DeCoster MA, Holger DK, Regenfuss MD.
389 1971 Experiments on the fluid mechanics of whistling. *J. Acoust. Soc.*
390 *Am.* **50**, 366–372. (doi:10.1121/1.1912641)
- 391 11. Shadle CH. 1983 Experiments on the acoustics of whistling. *Phys.*
392 *Teach.* **21**, 148–154. (doi:10.1119/1.2341241)
- 393 12. Henrywood RH, Agarwal A. 2013 The aeroacoustics of a steam kettle.
394 *Phys. Fluids* **25**, 107101. (doi:10.1063/1.4821782)
- 395 13. Sonntag CF. 1925 The comparative anatomy of the tongues of the
396 Mammalia. –XII. Summary, classification and phylogeny. *J. Zool.* **95**,
397 701–761.
- 398 14. Sanders I, Mu L. 2013 A three-dimensional atlas of human tongue
399 muscles. *Anat. Rec.* **296**, 1102–1114. (doi:10.1002/ar.22711)
- 400 15. Mu L, Sanders I. 2010 Human tongue neuroanatomy: Nerve supply and
401 motor endplates. *Clin. Anat.* **23**, 777–791. (doi:10.1002/ca.21011)

- 402 16. Weddell G, Harpman JA, Lambley DG, Young L. 1940 The innervation
403 of the musculature of the tongue. *J. Anat.* **74**, 255–267.
- 404 17. Stål P, Marklund S, Thornell LE, De Paul R, Eriksson P-O. 2003 Fibre
405 composition of human intrinsic tongue muscles. *Cells Tissues Organs*
406 **173**, 147–161. (doi:10.1159/000069470)
- 407 18. Vorperian HK, Kent RD. 2007 Vowel acoustic space development in
408 Children: A synthesis of acoustic and anatomic data. *J. Speech Lang.*
409 *Hear. Res.* **50**, 1510. (doi:10.1044/1092-4388(2007/104))
- 410 19. Stone M, Davis EP, Douglas AS, Aiver MN, Gullapalli R, Levine WS,
411 Lundberg AJ. 2001 Modeling tongue surface contours from cine-MRI
412 images. *J. Speech Lang. Hear. Res.* **44**, 1026. (doi:10.1044/1092-
413 4388(2001/081))
- 414 20. Story BH, Titze IR, Hoffman EA. 1996 Vocal tract area functions from
415 magnetic resonance imaging. *J. Acoust. Soc. Am.* **100**, 537–554.
416 (doi:10.1121/1.415960)
- 417 21. Titze IR. 2008 Nonlinear source–filter coupling in phonation: Theory. *J.*
418 *Acoust. Soc. Am.* **123**, 2733. (doi:10.1121/1.2832337)
- 419 22. Joliveau E, Smith J, Wolfe J. 2004 Tuning of vocal tract resonance by
420 sopranos. *Nature* **427**, 116.
- 421 23. Kaburagi T, Shimizu T, Uezu Y. 2018 A morphological and acoustic
422 analysis of the vocal tract during the act of whistling. *Acoust. Sci.*
423 *Technol.* **39**, 198–206. (doi:10.1250/ast.39.198)
- 424 24. Azola A, Palmer J, Mulheren R, Hofer R, Fischmeister F, Fitch WT.
425 2018 The physiology of oral whistling: A combined radiographic and
426 MRI analysis. *J. Appl. Physiol.* **124**, 34–39.
427 (doi:10.1152/jappphysiol.00902.2016)
- 428 25. Zhang S, Block KT, Frahm J. 2010 Magnetic resonance imaging in real
429 time: Advances using radial FLASH. *J. Magn. Reson. Imaging* **31**, 101–
430 109. (doi:10.1002/jmri.21987)
- 431 26. Audacity Team. 2018 Audacity(R): Free audio editor and recorder.
432 (v2.1.3). <http://audacityteam.org>
- 433 27. Boersma P, Weenink D. 2016 Praat: Doing phonetics by computer.
434 (v6.0.36). <http://www.fon.hum.uva.nl/praat/>
- 435
- 436 28. Mathworks. 2017 MATLAB. (R2017a). <https://www.mathworks.com/>
- 437 29. Correia JM. 2017 Online tongue segmentation using rtMRI.
438 http://github.com/joao-mendonca-correia/rtMRI_tongueTracking
- 439 30. Ramsay JO, Wickham H, Graves S, Hooker G. 2017 fda: Functional
440 Data Analysis.

- 441 31. R Core Team. 2019 R: A language and environment for statistical
442 computing. (v3.6.0) <http://cran.r-project.org/>.
- 443 32. Slud E, Stone M, Smith PJ, Goldstein M. 2002 Principal components
444 representation of the two-dimensional coronal tongue surface.
445 *Phonetica* **59**, 108–133. (doi:10.1159/000066066)
- 446 33. Ramsay JO, Hooker G, Spencer S. 2009 *Functional Data Analysis With*
447 *R and MATLAB*. New York: Springer Science+Business Media Inc.
- 448 34. Locantore N *et al.* 1999 Robust principal component analysis for
449 functional data. *Test* **8**, 1–73. (doi:10.1007/BF02595862)
- 450 35. Ramsay JO. 2000 Functional components of variation in handwriting. *J.*
451 *Am. Stat. Assoc.* **95**, 9–15. (doi:10.2307/2669518)
- 452 36. Levitin DJ, Nuzzo RL, Vines BW, Ramsay JO. 2007 Introduction to
453 functional data analysis. *Can. Psychol. Can.* **48**, 135–155.
454 (doi:10.1037/cp2007014)
- 455 37. Bates D, Maechler M, Bolker B, Walker S. 2015 Fitting linear mixed-
456 effects models using lme4. *J. Stat. Softw.* **67**, 1–48.
457 (doi:10.18637/jss.v067.i01)
- 458 38. Barr DJ, Levy R, Scheepers C, Tily HJ. 2013 Random effects structure
459 for confirmatory hypothesis testing: Keep it maximal. *J. Mem. Lang.* **68**,
460 255–278. (doi:10.1016/j.jml.2012.11.001)
- 461 39. Rakerd B, Verbrugge RR. 1985 Linguistic and acoustic correlates of the
462 perceptual structure found in an individual differences scaling study of
463 vowels. *J. Acoust. Soc. Am.* **77**, 296–301. (doi:10.1121/1.392393)
- 464 40. Hillenbrand J, Getty LA, Clark MJ, Wheeler K. 2005 Acoustic
465 characteristics of American English vowels. *J. Acoust. Soc. Am.* **97**,
466 3099–3111. (doi:10.1121/1.411872)
- 467 41. Adank P, Hout R Van, Smits R. 2004 An acoustic description of the
468 vowels of Northern and Southern Standard Dutch. *J. Acoust. Soc. Am.*
469 **116**, 1729–1738. (doi:10.1121/1.1779271)
- 470 42. Heald SLM, Nusbaum HC. 2015 Variability in vowel production within
471 and between days. *PLoS One* **10**, 1–14.
472 (doi:10.1371/journal.pone.0136791)
- 473 43. Bernstein NA. 1967 *The co-ordination and regulation of movements*.
474 Oxford: Pergamon Press.
- 475 44. Classe A. 1957 The unusual whistle language of the Canary Islanders:
476 ‘Bring me two horses’, he whistled. *UNESCO Cour.* **11**, 30–32.
- 477 45. Busnel RG. 1964 Document sur une langue sifflée Pyrénéenne.
- 478 46. Güntürkün O, Güntürkün M, Hahn C. 2015 Whistled Turkish alters
479 language asymmetries. *Curr. Biol.* **25**, R706–R708.

- 480 (doi:10.1016/j.cub.2015.06.067)
- 481 47. Charalambakis C. 1994 A case of whistled speech from Greece. In
482 *Themes in Greek linguistics: Papers from the 1st International*
483 *Conference on Greek Linguistics* (eds I Philippaki-Warburton, K
484 Nicolaidis, M Sifianous), pp. 389–396. Amsterdam & Philadelphia:
485 Benjamins.
- 486 48. Belyk M, Johnson JF, Kotz SA. 2018 Poor neuro-motor tuning of the
487 human larynx: A comparison of sung and whistled pitch imitation. *R.*
488 *Soc. Open Sci.* **5**, 171544. (doi:10.1098/rsos.171544)
- 489 49. Lameira AR, Hardus ME, Kowalsky B, de Vries H, Spruijt BM, Sterck
490 EHM, Shumaker RW, Wich SA. 2013 Orangutan (*Pongo* spp.) whistling
491 and implications for the emergence of an open-ended call repertoire: A
492 replication and extension. *J. Acoust. Soc. Am.* **134**, 2326–2335.
493 (doi:10.1121/1.4817929)
- 494 50. Wich SA, Swartz KB, Hardus ME, Lameira AR, Stromberg E, Shumaker
495 RW. 2009 A case of spontaneous acquisition of a human sound by an
496 orangutan. *Primates* **50**, 56–64. (doi:10.1007/s10329-008-0117-y)
- 497 51. Fitch WT, de Boer B, Mathur N, Ghazanfar AA. 2016 Monkey vocal
498 tracts are speech-ready. *Sci. Adv.* **2**, e1600723.
499 (doi:10.1126/sciadv.1600723)
- 500